ELSEVIER

Flow Regime Map for a Horizontal Pipe with Uniform Wall Heat Flux and Three Inlet Configurations

Afshin J. Ghajar
Lap-Mou Tam
School of Mechanical and Aerospace Engineering, Oklahoma State University, Stillwater, Oklahoma

■A flow regime map for determination of the boundary between forced and mixed convection in a horizontal circular straight tube with reentrant, square-edged, and bell-mouth inlets under uniform wall heat flux boundary condition is developed. The flow regime map is applicable to all flow regimes (laminar, transition, turbulent). From the flow regime map, for any forced flow represented by a given Reynolds number, the value of the parameter Gr Pr at a particular x/D location indicates whether it is necessary to consider buoyancy effects. For the identified pure forced or mixed convection heat transfer regime, a heat transfer correlation is recommended.

Keywords: *flow regime map, forced convection, mixed convection, transition region, circular tube, uniform wall heat flux*

INTRODUCTION

Heating a fluid flowing in a horizontal pipe produces a secondary flow. The fluid near the pipe wall, due to its higher temperature and lower density, circulates upward, while the fluid near the central region of the pipe, having a lower temperature and a higher density, circulates downward. These counterrotating transverse vortices that are superimposed on the streamwise main flow due to free convection effects (buoyancy influences) can significantly increase the forced convection heat transfer. It is important to realize that heat transfer in combined forced and free (or mixed) convection can be significantly different from its values in both pure free and pure forced convection. Actually, buoyancy forces (free convection effects) are present in any forced convection flow, and for design purposes it is of interest to know when they can be neglected and when they have to be accounted for. Such an investigation is made difficult by the large number of influencing parameters. Buoyancy influences forced convection heat transfer in horizontal pipes in ways that depend on Reynolds, Prandtl, and Grashof numbers as well as the pipe inlet configuration, wall boundary condition, and the length-to-diameter ratio of the pipe [1]. This makes it difficult and sometimes even dangerous to make a priori assumptions concerning buoyancy effects in internal flow.

Metais and Eckert [2] recommended the use of the flow regime map of Fig. 1 for determining the boundary between mixed and forced convection in horizontal pipes under uniform wall temperature boundary conditions. For the identified pure forced or mixed convection heat transfer regime, a heat transfer correlation for the laminar or turbulent flow is offered on the map. In Fig. 1, the flow regime boundary was arbitrarily determined to be the location where the mixed convection heat transfer does not deviate by more than 10% from pure forced convection. From the flow regime map, for any forced flow represented by a given Reynolds number, the value of the parameter Gr Pr D/x indicates whether it is necessary to consider buoyancy effects. The shaded area of Fig. 1 is the transition region. Based on the experimental results of Kern and Othmer [3], Metais [4] determined the transition Reynolds number range between the laminar and turbulent mixed convection regions to be between 600 and 800. The transition Reynolds number range between laminar and turbulent forced convection from the figure appears to be between 2000 and 3100. However, Metais [4] did not report the source of this information. Also note that, due to lack of experimental data, the figure does not show a boundary between free and mixed convection regions. It should be noted that there is no flow regime map comparable to Fig. 1 for the case of uniform wall heat flux boundary condition. In fact, the influence of gravity (buoyancy effect) on forced convection is stronger with an imposed uniform wall heat flux boundary condition than with the uniform wall temperature boundary condition and the response is greater when the flow is horizontal than when it is vertical.

It would be of great interest to show the applicability of the flow regime map given in Fig. 1 for uniform wall

Address correspondence to Professor A. J. Ghajar, School of Mechanical and Aerospace Engineering, Oklahoma State University, Stillwater, OK 74078.

Experimental Thermal and Fluid Science 1995; 10:287–297

655 Avenue of the Americas, New York, NY 10010

0894-1777/95/$9.50
SSDI 0894-1777(94)00107-J

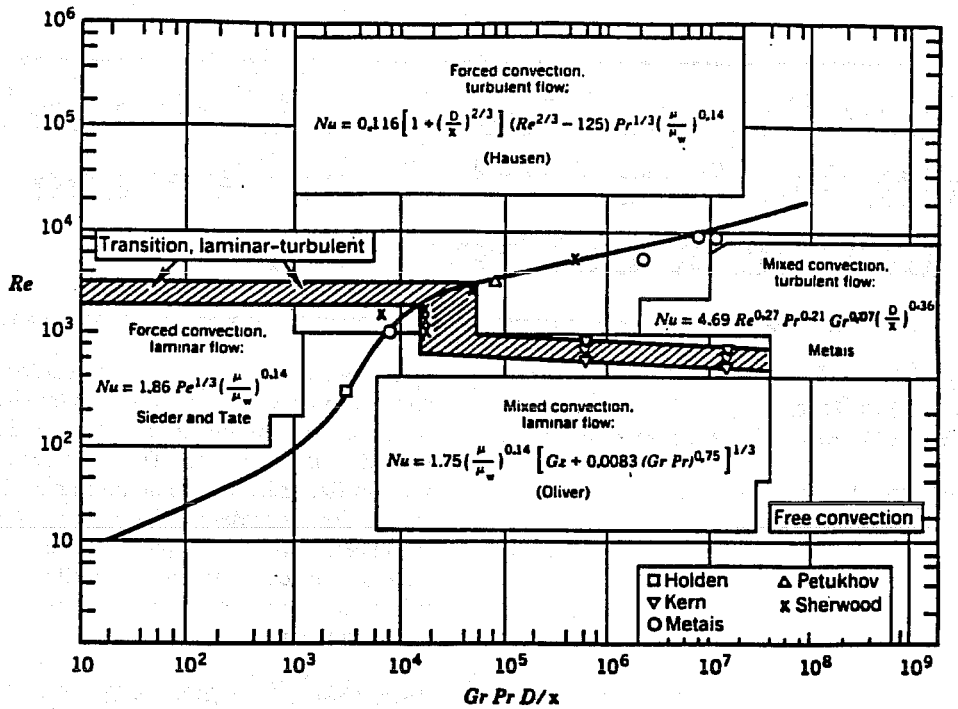

Figure 1. Free, forced, and mixed convection regimes for flow in horizontal circular tubes for $10^{-2} < \mathrm{Pr}\, D/x < 1$ and uniform wall temperature boundary condition, taken from Aung [10].

temperature to our recent laminar-transitional-turbulent forced and mixed convection experimental data obtained in a horizontal pipe with uniform wall heat flux and three different inlet configurations (reentrant, square-edged, and bell-mouth) (see Ghajar and Tam [1]). For this purpose, Fig. 1 has been replotted as Fig. 2 with only the parameter Gr Pr in the abscissa. According to Metais and Eckert [2], for flow through horizontal tubes, as long as $10^{-2} < \mathrm{Pr}\, D/x < 1$, D/x need not be included in the abscissa. Figure 2 shows a comparison of our experimental data with uniform wall heat flux for reentrant, square-edged, and bell-mouth inlets with Metais and Eckert's flow regime map for uniform wall temperature. Because of the type of fluid used in these experiments (distilled water and mixtures of distilled water and ethylene glycol), the experimental data do not cover the free convection and mixed turbulent convection regions. The figure shows that all the forced turbulent convection data are predicted correctly by the Metais–Eckert flow regime map. However, the experimental data for forced laminar, mixed laminar, mixed transition, and forced transition were not predicted correctly. The reason for this discrepancy is mainly the influence of boundary condition (uniform wall temperature vs. uniform wall heat flux) and inlet geometry. In the laminar and lower transition regions, the type of boundary condition has a significant influence on the heat transfer characteristics of the flow. Therefore, it is reasonable to expect the flow regime map developed based on uniform wall temperature boundary condition not to do a good job in predicting uniform wall heat flux data. On the other hand, the turbulent data are insensitive to the boundary condition and, as shown in Fig. 2, the flow regime map predicts the data properly. As reported in our previous works [1, 5], the type of inlet configuration influences the start and end of the transition region and the starting length necessary for the establishment of the free convection effects. This is another reason why the forced and mixed laminar and transition data were not predicted correctly by the flow regime map.

The objective of this study was to construct a flow regime map similar to the one developed for uniform wall temperature by Metais and Eckert [2]. For this purpose, our recent uniform wall heat flux heat transfer data and correlations for a horizontal pipe with three different inlets were used [1].

HEAT TRANSFER EXPERIMENTS

The heat transfer experimental data used in this study along with a detailed description of the experimental apparatus and procedures used were reported by Ghajar and Tam [1]. In this paper only a brief description of the experimental setup and procedures will be provided. The local forced and mixed convective heat transfer measurements were made in a horizontal electrically heated stainless steel circular straight tube with reentrant, square-edged, and bell-mouth inlets under uniform wall heat flux condition. The pipe had an inside diameter of 1.58 cm and an outside diameter of 1.90 cm. The total length of the test section was 6.10 m, which provided a maximum length-to-diameter ratio (L/D) of 385. A uniform wall heat flux boundary condition as maintained by a dc arc welder. Thermocouples (T-type) were placed on the outer surface of the tube wall at close intervals near the entrance and at greater intervals further downstream. Twenty-six axial locations were designated, with four thermocouples placed at each location. The thermocouples were placed 90° apart around the periphery. From the local peripheral wall temperature measurements at each axial location, the inside wall temperatures and the local heat transfer coefficients were calculated using a data reduction computer program [6]. In these calculations, axial conduction was assumed negligible (Re Pr > 42,000 in all cases), but peripheral and radial conduction of heat

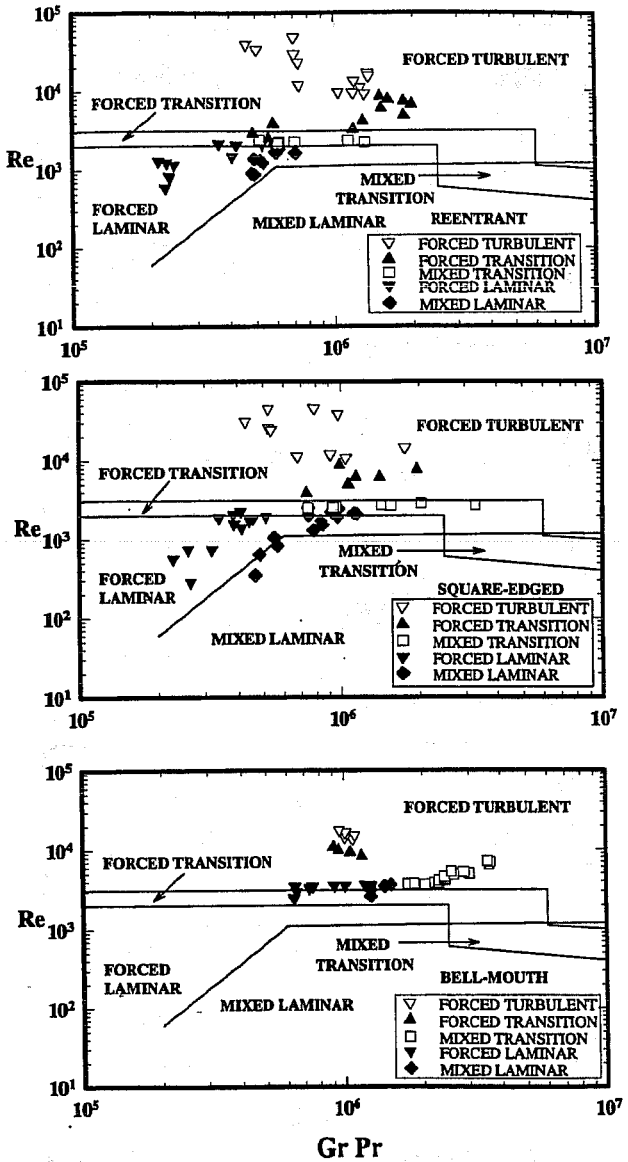

Figure 2. Comparison of Metais and Eckert's [2] flow regime map with experimental data [1] for uniform wall heat flux and three different inlet configurations.

in the tube wall were included. In addition, the bulk fluid temperature was assumed to increase linearly from the inlet to the outlet. As reported by Ghajar and Tam [1], the uncertainty analyses of the overall experimental procedures showed that there is a maximum of 9% uncertainty for the heat transfer coefficient calculations.

To ensure a uniform velocity distribution in the test fluid before it entered the test section, the flow passed through calming and inlet sections. The calming section had a total length of 61.6 cm and consisted of a 17.8-cm-diameter acrylic cylinder with three perforated acrylic plates followed by tightly packed soda straws sandwiched between galvanized steel mesh screens [1]. Before entering the inlet section, the test fluid passed through a fine mesh screen and flowed undisturbed through 23.5 cm of a 16.5-cm-diameter acrylic tube before it entered the test section. The inlet section had the versatility of being modified to incorporate a reentrant or bell-mouth inlet (see Fig. 3). The reentrant inlet was simulated by sliding 1.91 cm of the tube entrance length into the inlet section, which was otherwise the square-edged (sudden contraction) inlet. For the bell-mouth inlet, a fiberglass nozzle with a contraction ratio of 10.7 and a total length of 23.6 cm was used in place of the inlet section.

In the experiments, distilled water and mixtures of distilled water and ethylene glycol were used. The experiments covered the local bulk Reynolds number range 280–49,000, the local bulk Prandtl number range 4–158, the local bulk Grashof number range 1000–2.5×10^5, and the local bulk Nusselt number range 13–258. The wall heat flux for the experiments ranged from 4 to 670 kW/m^2.

FORCED AND MIXED CONVECTION HEAT TRANSFER BOUNDARY

Application of heat to the tube wall produces a temperature difference in the fluid. This temperature difference may produce a secondary flow due to free convection. The boundary between mixed and forced convection can be determined from the local heat transfer data. The ratio of the local peripheral heat transfer coefficient at the top of the tube to the local peripheral heat transfer coefficient at the bottom of the tube (h_t/h_b) should be close to unity (0.8–1.0) for forced convection and is much less than unity (< 0.8) for a case in which mixed convection exists [1, 5]. Mixed convection heat transfer, in addition to being dependent on Reynolds and Prandtl numbers, is also dependent upon the Grashof number (which accounts for the variation in density of the test fluid).

To illustrate and explain the different heat transfer modes (mixed and forced convection) encountered for the three inlets during the experiments, Fig. 4 is presented. This figure shows the different trends in the heat transfer coefficient ratio h_t/h_b. It includes representative Reynolds number ranges from laminar to fully turbulent flow for the three inlets (Re = 280–49,000). As shown in the figure, the boundary between forced and mixed convection heat transfer is inlet-dependent. For the reentrant, square-edged, and bell-mouth inlets, when the Reynolds number was greater than 2500, 3000, and 8000, respectively, the flows were dominated by forced convection heat transfer and the heat transfer coefficient ratios did not fall below 0.8–0.9 and at times exceeded unity due to roundoff errors in the property evaluation subroutine of the data reduction program [6]. The flows dominated by mixed convection heat transfer had heat transfer coefficient ratios beginning near 1 but dropping off rapidly as the length-to-diameter ratio increased. Beyond about 125 diameters from the tube entrance, the ratio was almost invariant with x/D, indicating a much less dominant role for forced convection heat transfer and an increased free convection activity.

In reference to Fig. 4, it is interesting to observe that the starting length necessary for the establishment of the free convection effect for low Reynolds number flows was also inlet-dependent. When the secondary flow was established, a sharp decrease in h_t/h_b occurred. Depending on the type of inlet configuration, for low Reynolds number flows (Re < 2500 for reentrant, Re < 3000 for square-edged, and Re < 8000 for bell-mouth), the flow can be considered to be dominated by forced convection over the

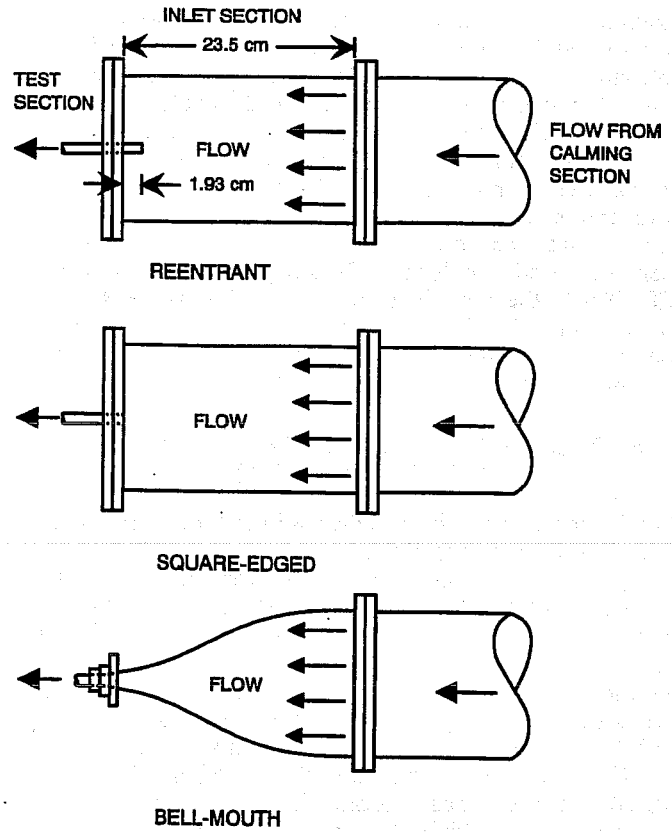

Figure 3. Schematic of the three different inlet configurations.

first 20–70 diameters from the entrance to the tube. As pointed out earlier in reference to Fig. 1, these influences of the inlet configuration on the establishment of the secondary flow in horizontal pipes were also not included in the flow regime map of Metais and Eckert, and this is another reason why some of our mixed laminar and transitional experimental data were not predicted correctly by their flow regime map (see Fig. 2).

INFLUENCE OF INLET ON HEAT TRANSFER TRANSITION REGION

Figure 5 clearly shows the influence of inlet configuration on the beginning and end of the heat transfer transition region. This figure plots the local average peripheral heat transfer coefficients in terms of the Colburn j factor ($St\,Pr^{0.67}$) versus local bulk Reynolds number for all flow regimes at the length-to-diameter ratio of 192. The filled symbols represent the start and end of the heat transfer transition region for each inlet configuration. According to Fig. 5, the heat transfer transition Reynolds number range for our experimental data is different from that used by Metais and Eckert [2] in Fig. 1 (shaded area). For this reason, some of our forced and mixed transition data were not predicted properly by the transition region of the flow regime map (see Fig. 2). This indicates that the influence of the type of inlet on the start and end of the heat transfer transition region was not taken into consideration in their flow regime map.

Figure 5, for comparison purposes, also shows the typical fully developed pipe flow forced convection heat transfer correlations for turbulent [7] and laminar (Nu = 4.364) flows under the uniform wall heat flux boundary condition. In the turbulent flow regime, for Reynolds numbers greater than about 8500–10,500 (depending on the inlet type), the experimental data appear on the turbulent heat transfer line (within ±8%). However, in the laminar flow regime, for Reynolds numbers less than about 2000–3800 (depending on the inlet type), the data appear to have a pronounced and almost parallel shift above the accepted laminar heat transfer line. This is directly due to the strong influence of buoyancy forces (free convection) on forced convection, giving rise to mixed convection heat transfer. This in turn results in a higher fully developed laminar uniform wall heat flux Nusselt number than the accepted 4.364 value (a value of about 14.5 is estimated for the data). It should be noted that in the fully developed laminar flow region no forced convection data could be obtained. At the minimum welder current setting (approximately 150 A), the heat generated at the tube wall

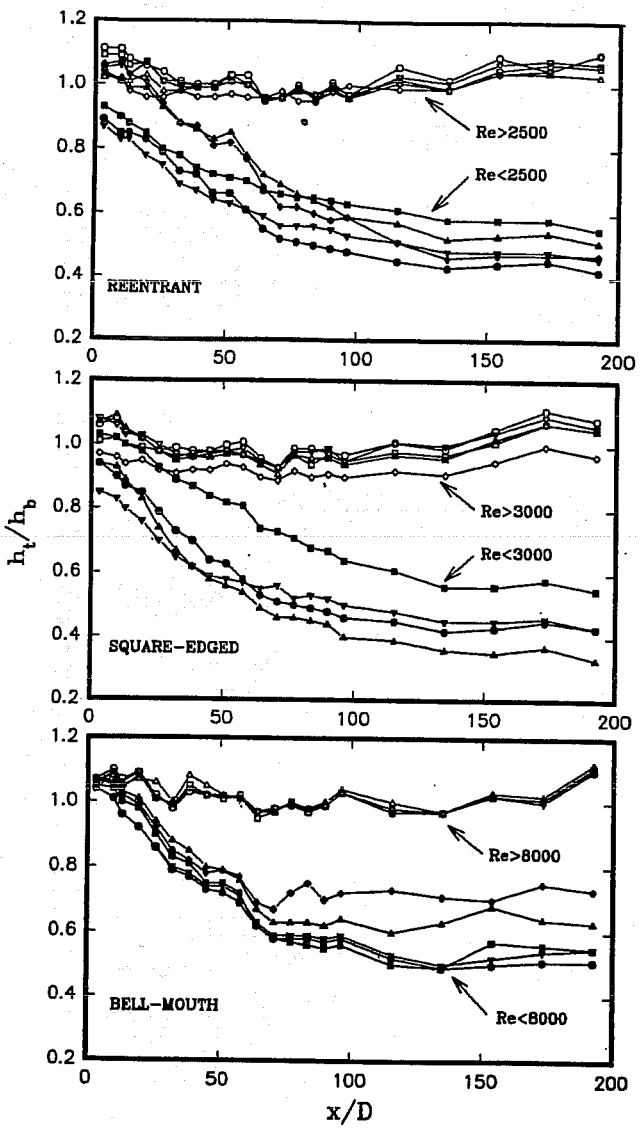

Figure 4. Effect of secondary flow on heat transfer coefficient for different inlet configurations and flow regimes.

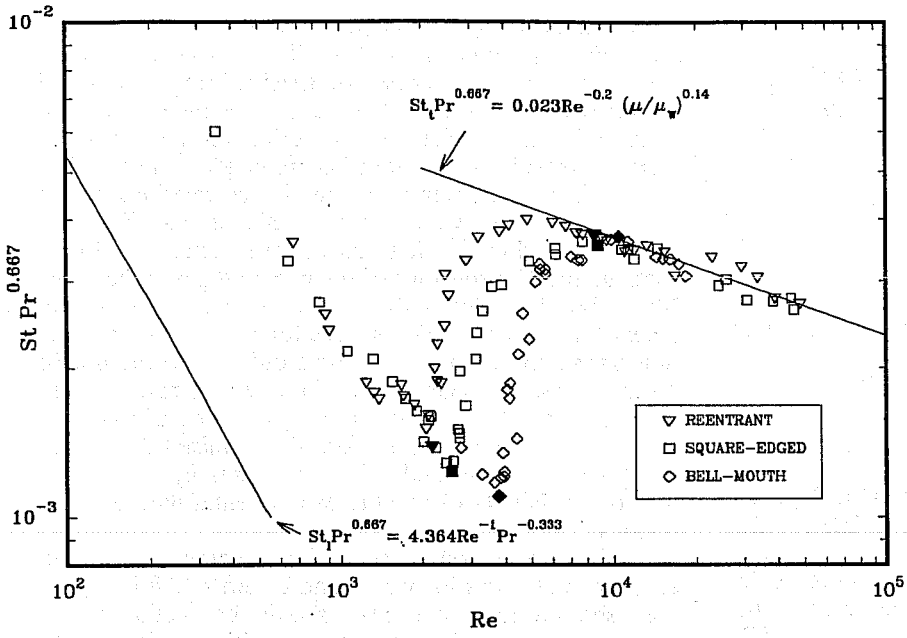

Figure 5. Influence of different inlet configurations on heat transfer transition region at $x/D = 192$. (The solid symbols indicate the start and end of the transition region.)

was enough to bring about peripheral temperature variations extensive enough to cause secondary flow.

As shown by the filled symbols in Fig. 5, the lower and upper limits of heat transfer transition Reynolds number range depend on inlet configuration. In addition, these transition Reynolds number limits are x/D-dependent, and they increase with an increase in x/D. This increase in the transition limits is solely due to variation of physical properties along the pipe. In this case, the increase in the wall and fluid bulk temperatures along the pipe causes the fluid kinematic viscosity to decrease with an increase in x/D. This in turn causes the local bulk Reynolds number (i.e., lower and upper limits of heat transfer transition Reynolds number range) to increase along the pipe. To determine the range of heat transfer transition Reynolds numbers along the pipe ($3 \leq x/D \leq 192$), figures similar to Fig. 5 were developed for 20 other x/D locations. From these figures, the heat transfer transition Reynolds number range for each inlet was determined to be about 2000–8500 for the reentrant inlet, 2400–8800 for the square-edged inlet, and 3400–10,5000 for the bell-mouth inlet. Figure 6 depicts the variation of the lower and the upper limits of heat transfer transition Reynolds numbers along the pipe for each inlet. Since the heat transfer transition limits vary linearly with x/D along the pipe, they were curve-fitted with the following linear equations for each inlet:

1. Reentrant

$$\begin{aligned} &\text{Lower bound:} && \text{Re} = 2157 - 0.65(192 - x/D) \\ &\text{Upper bound:} && \text{Re} = 8475 - 9.28(192 - x/D) \end{aligned} \quad \textbf{(1a)}$$

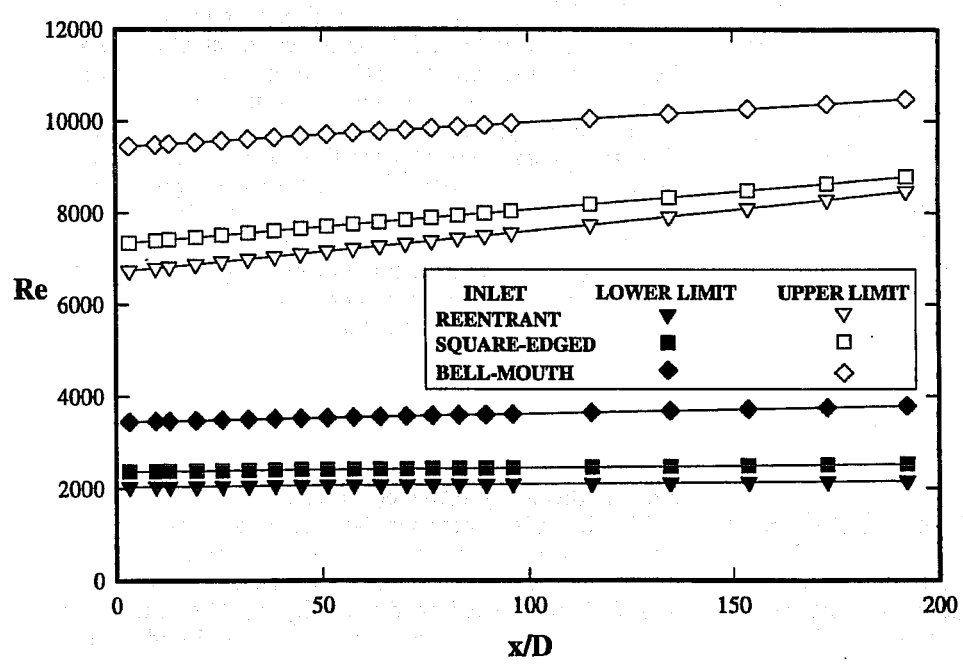

Figure 6. Variation of the lower and the upper limits of heat transfer transition Reynolds number along the pipe for three different inlet configurations.

2. Square-edged

$$\begin{aligned} &\text{Lower bound:} && \mathrm{Re} = 2524 - 0.82(192 - x/D) \\ &\text{Upper bound:} && \mathrm{Re} = 8791 - 7.69(192 - x/D) \end{aligned} \quad (1b)$$

3. Bell-mouth

$$\begin{aligned} &\text{Lower bound:} && \mathrm{Re} = 3787 - 1.80(192 - x/D) \\ &\text{Upper bound:} && \mathrm{Re} = 10481 - 5.47(192 - x/D) \end{aligned} \quad (1c)$$

The average absolute deviations for the linear equations (1a)–(1c) in all cases were less than 0.16%.

The above equations for the heat transfer transition Reynolds numbers indicate that the inlet that caused the most disturbance (reentrant) produced an early transition (Re = 2000), and the inlet with the least disturbance (bell-mouth) did not go into transition below a Reynolds number of about 3500. The square-edged inlet, which causes less disturbance than the reentrant inlet but more than the bell-mouth inlet, produced a transition Reynolds number of about 2400. It should be pointed out that the reported lower (at $x/D = 3$) and upper (at $x/D = 192$) limits of heat transfer transition Reynolds numbers are not influenced by the presence of mixed convection (see Fig. 4). However, as the flow travels the pipe length required for the establishment of secondary flow, the beginning of the transition region will be influenced by the presence of mixed convection.

FLOW REGIME MAP

In Metais and Eckert's [2] flow regime map shown in Fig. 1, the boundary between laminar forced and mixed convection regions was apparently based on the correlations of either Kern and Othmer [3] or Eubank and Proctor [8]. Metais [4], in his report, gave no clear explanation as to which correlation was used. In the turbulent region, the boundary between forced and mixed convection regions was based on the correlations of Metais and Kraussold (see Metais [4]). In the development of the flow regime map, Metais and Eckert [2] used the mentioned laminar and turbulent forced and mixed convection correlations with the general relationship

$$\mathrm{Nu}_{\mathrm{mixed}} = \mathrm{Nu}_{\mathrm{forced}} \times \text{correction factor}. \quad (2)$$

The correction factor (F) is a function of Gr, Pr, and Re. To find the boundary between forced and mixed convection regions, Metais and Eckert [2] arbitrarily set the correction factor to 10%. In other words, $\mathrm{Nu}_{\mathrm{mixed}}$ was set to be 10% greater than $\mathrm{Nu}_{\mathrm{forced}}$. In this fashion, Eq. (2) becomes

$$\mathrm{Nu}_{\mathrm{mixed}}/\mathrm{Nu}_{\mathrm{forced}} = 1.1 = F(\mathrm{Gr}, \mathrm{Pr}, \mathrm{Re}). \quad (3)$$

Equation (3) can be rearranged so that the Reynolds number can be represented as a function of the Grashof and Prandtl numbers, or

$$\mathrm{Re} = f(\mathrm{Gr}, \mathrm{Pr}). \quad (4)$$

Equation (4) represents the general form of the expression used by Metais [4] to develop equations for the boundaries between the laminar and turbulent forced and mixed convection regions. These equations are represented in Fig. 1 by the solid line. In reference to Fig. 1, it is also interesting to note that although the solid line separating the laminar and turbulent forced and mixed convection regions was based on specific forced and mixed convection heat transfer correlations, only one of the correlations used (Metais's correlation for the turbulent mixed convection) has been recommended on the flow regime map. The other recommended correlations on the flow regime map were those of Sieder and Tate for laminar forced convection, Oliver for laminar mixed convection, and Hausen for turbulent forced convection (see Metais [4]). In addition, the flow regime map doesn't offer a heat transfer correlation for the forced or mixed convection transition regions. As pointed out earlier, the details on the transition region in the flow regime map (shaded area) are very sketchy, and the reported transition Reynolds number ranges in the forced and mixed convection regions are not justified. This was primarily due to the lack of availability of reliable experimental data in these regions.

As discussed in reference to Fig. 2, comparison of our experimental data with Metais and Eckert's [2] flow regime map showed that their map should be modified. The dependency of the heat transfer transition region on the type of inlet configuration should be incorporated into the flow regime map, and the boundary between laminar and transition forced and mixed convection regions should be redefined. For this purpose, our experimental data for the three inlets were used [1].

Development of the new boundary required laminar and transition forced and mixed convection data. As pointed out in reference to Fig. 4, secondary flow needs a certain length for development. Our experimental data indicated that for $x/D < 70$, pure forced convection is still dominant in the laminar and lower transition regions. The experimental data for development of this new boundary between laminar and transition forced and mixed convection regions can be identified by using the criterion that the ratio of the local peripheral heat transfer coefficient at the top of the tube to the local peripheral heat transfer coefficient at the bottom of the tube (h_t/h_b) should be greater than or equal to 0.8 for forced convection and less than 0.8 for mixed convection (see Fig. 4). This way, 51 data points that represent the boundary between laminar and transition forced and mixed convection for the three inlets used in our experiments were identified. Figure 7 shows the data points plotted on the flow regime map coordinates (Re vs. Gr Pr). To obtain a smooth boundary between the laminar and transition forced and mixed convection regions, the data points for the three inlets were curve-fitted in the form given by Eq. (4) using a least squares curve-fitting program. The recommended equation for the forced and mixed convection regions in the flow regime map is

$$\mathrm{Re} = 2674 + 5.35 \times 10^{-13}(\mathrm{Gr}\,\mathrm{Pr})^{2.5} - 1.85 \times 10^{-16}(\mathrm{Gr}\,\mathrm{Pr})^{3} - 2.64 \times 10^{14}(\mathrm{Gr}\,\mathrm{Pr})^{-2}. \quad (5)$$

Equation (5) correlates the 51 data points with a correlation coefficient of 0.96 (see Fig. 7).

The boundary between laminar and transition forced and mixed convection regions given in Metais and Eckert's [2] original flow regime map (see Fig. 1) and replotted as Fig. 2 should be replaced with Eq. (5) when the uniform wall heat flux boundary condition is used. In addition, the

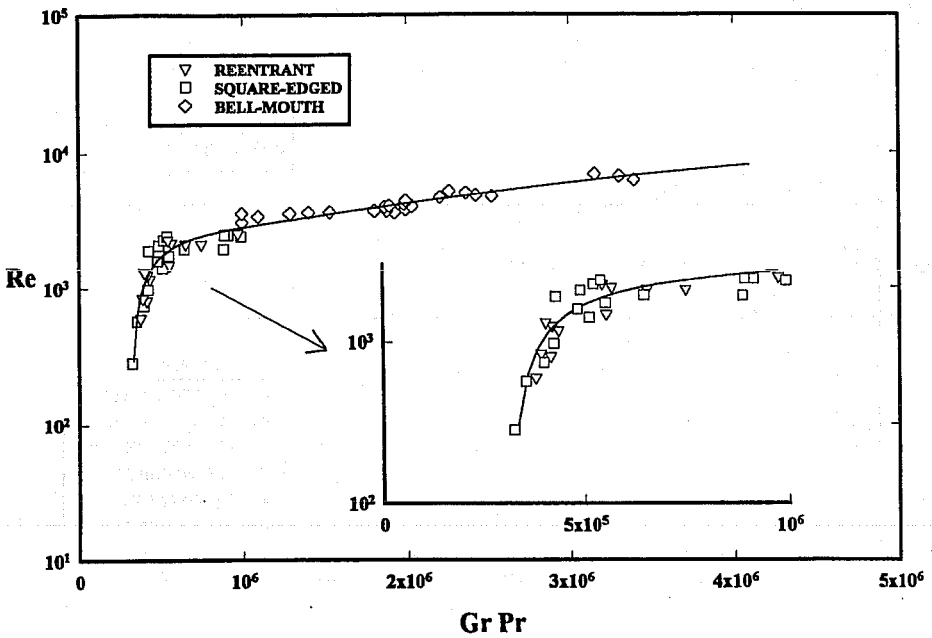

Figure 7. The boundary between forced and mixed convection.

heat transfer transition Reynolds number ranges for the three inlets should be incorporated into the flow regime map. These changes appear in the revised version of the flow regime map given as Fig. 8. In this figure there is a common boundary for all three inlets separating the laminar forced and mixed convection regions. However, for the transition forced and mixed convection regions, the boundaries depend on the inlet configuration. The lower and upper bounds of heat transfer transition Reynolds numbers for each inlet shown in Fig. 8 were based on the results at $x/D = 3$ and 192, respectively. For other x/D locations, based on Eqs. (1a)–(1c), a slight adjustment for each inlet might be necessary.

The proposed flow regime map (see Fig. 8) was verified with our experimental data for the three inlets. The results of these comparisons are shown in Figs. 9, 10, and 11 for the reentrant, square-edged, and bell-mouth inlets, respectively. As shown in these figures, the experimental data for all applicable flow regimes are predicted correctly by the revised flow regime map. In addition, Fig. 12 shows an independent check of the revised flow regime map with experimental data of Chen [9] for a square-edged inlet. Again, the revised flow regime map predicted the flow regimes correctly.

HEAT TRANSFER CORRELATIONS

From the revised flow regime map (see Fig. 8), for any forced flow represented by a given Reynolds number, the value of parameters Gr Pr at a particular x/D location indicates whether it is necessary to consider buoyancy effects. Once the forced convective mode of heat transfer

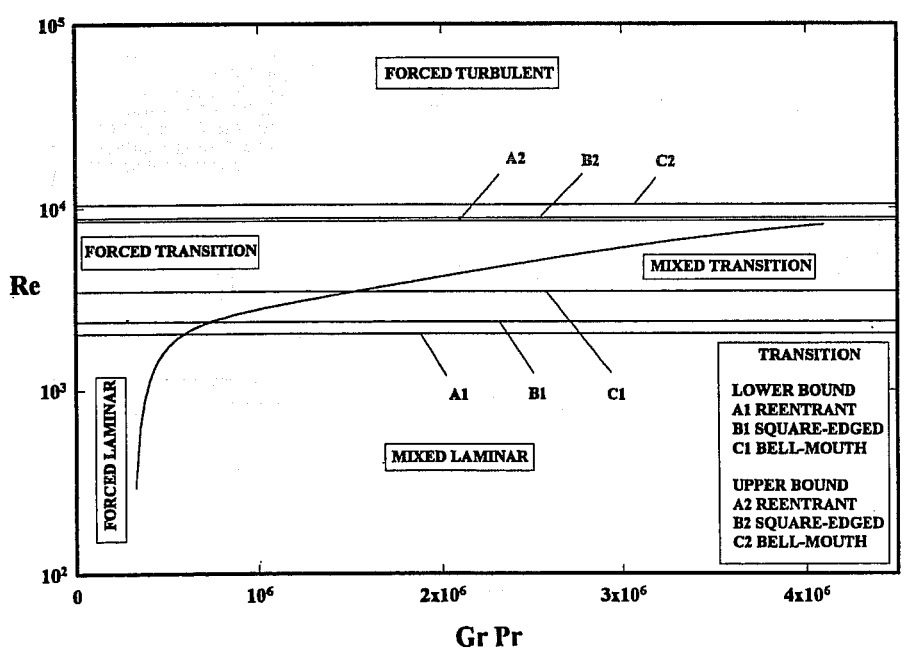

Figure 8. The new flow regime map for flow in horizontal tubes with three different inlet configurations and uniform wall heat flux.

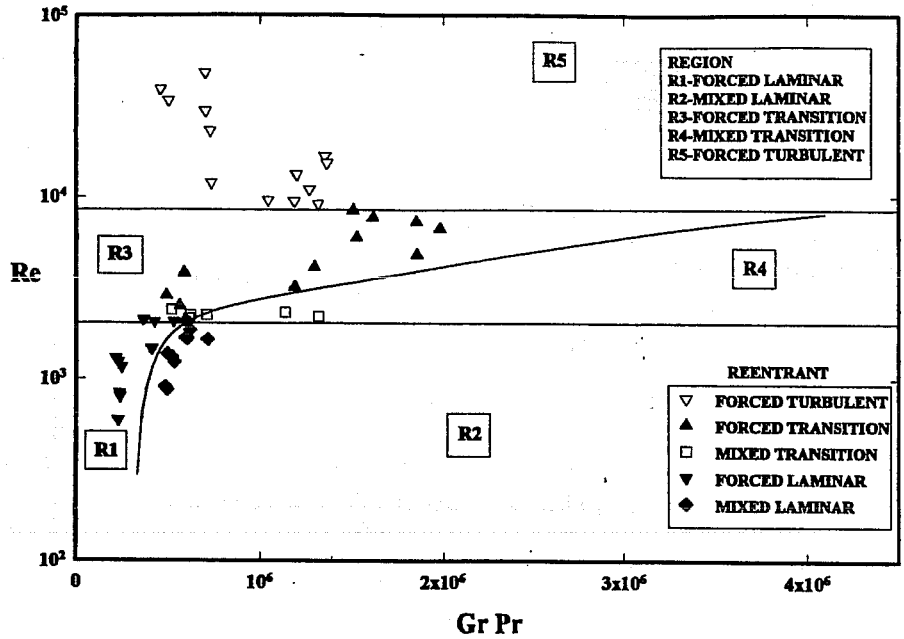

Figure 9. Comparison of experimental data of [1] for a reentrant inlet with the new flow regime map.

(pure or mixed) for a particular flow regime (laminar-transition-turbulent) is determined, the heat transfer coefficient can be calculated from an appropriate heat transfer correlation. For the flow regime map proposed in Fig. 8, the following heat transfer correlations, which were developed by Ghajar and Tam [1], are recommended. Further details on these correlations may be found in [1].

Laminar Region

$$\mathrm{Nu}_1 = 1.24\left[(\mathrm{Re\,Pr}\,D/x) + 0.025(\mathrm{Gr\,Pr})^{0.75}\right]^{1/3} \times(\mu/\mu_w)^{0.14}, \quad (6)$$

where

$$3 \le x/D \le 192, \quad 280 \le \mathrm{Re} \le 3800, \quad 40 \le \mathrm{Pr} \le 160,$$
$$1000 \le \mathrm{Gr} \le 2.8 \times 10^4, \quad 1.2 \le \mu/\mu_w \le 3.8.$$

Equation (6) is applicable to laminar forced and mixed convection in the entrance and fully developed regions and can be used for all three inlets. The equation gave a representation of the experimental data to within +15.4% and −16.9%. In the development of the correlation, a total of 546 experimental data points were used. The absolute average deviation between the results predicted by the correlation and the experimental data was 5.8%. About 14% of the data (78 data points) were predicted with more than ±10% deviation, and 86% of the data (468 data points) with less than ±10% deviation.

Turbulent Region

$$\mathrm{Nu}_t = 0.023\,\mathrm{Re}^{0.8}\,\mathrm{Pr}^{0.385}(x/D)^{-0.0054}(\mu/\mu_w)^{0.14}, \quad (7)$$

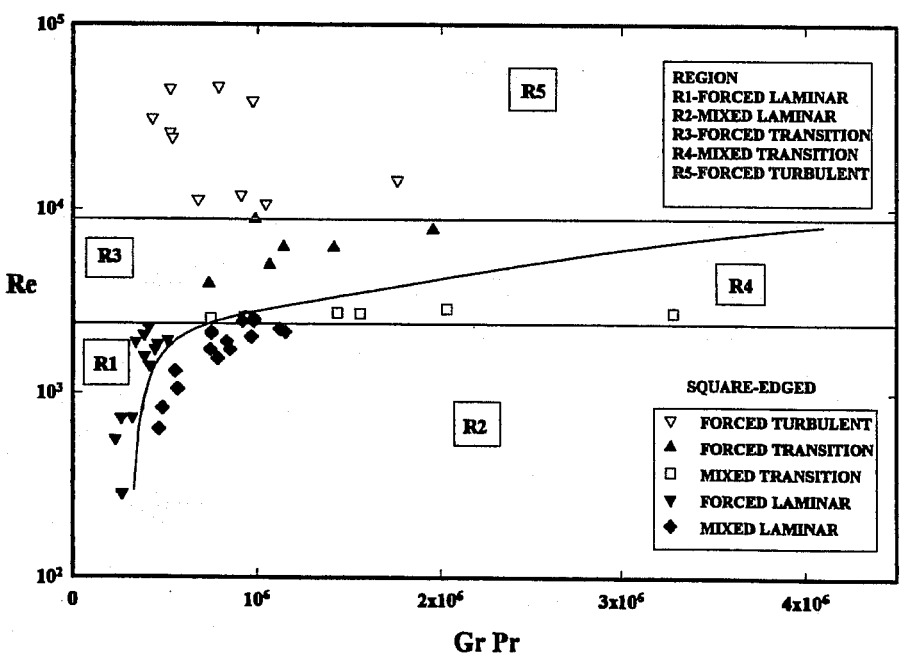

Figure 10. Comparison of experimental data of [1] for a square-edged inlet with the new flow regime map.

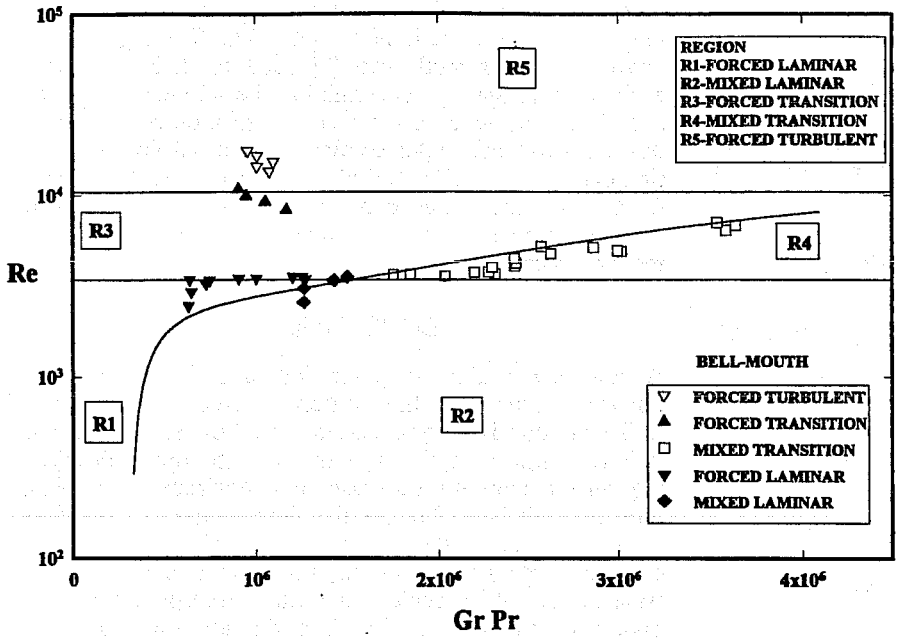

Figure 11. Comparison of experimental data of [1] for a bell-mouth inlet with the new flow regime map.

where

$$3 \le x/D \le 192, \qquad 7000 \le \mathrm{Re} \le 49{,}000,$$

$$4 \le \mathrm{Pr} \le 34, \qquad 1.1 \le \mu/\mu_w \le 1.7.$$

Equation (7) is applicable to turbulent forced convection in the entrance and fully developed regions and can be used for all three inlets. The equation correlated the experimental data to within $+10.5\%$ and -10.3%. Due to the type of fluid used in our experiments, our data in this region were free from buoyancy effects. The flow in this region (turbulent mixed convection) is insensitive to the type of wall boundary condition (uniform wall heat flux or temperature). Therefore, Metais and Eckert's [2] original flow regime map and correlation for turbulent mixed convection can still be used. In the development of the correlation, 604 experimental data points were used. The absolute average deviation between the results predicted by the correlation and the experimental data was 3.7%. The correlation predicted 93% of the experimental data (600 data points) by less than $\pm 10\%$ deviation and 73% of the data with less than $\pm 5\%$ deviation.

Transition Region In the transition region, flow has both laminar and turbulent characteristics. In addition, the type of inlet configuration influences the beginning and end of the transition region. Thus a single correlation for this region cannot predict the data, and a correlation for each inlet should be developed. The form of the

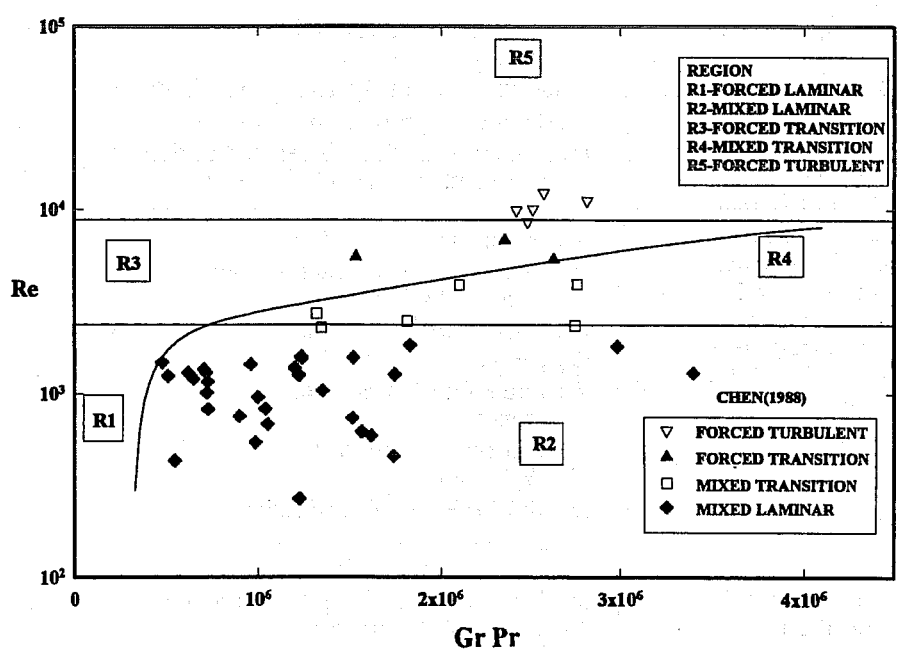

Figure 12. Comparison of experimental data of [9] for a square-edged inlet with the new flow regime map.

correlation developed for this region is

$$\mathrm{Nu}_{tr} = \mathrm{Nu}_l + \left\{\exp\left[\frac{a - \mathrm{Re}}{b}\right] + \mathrm{Nu}_t^c\right\}^c, \qquad (8)$$

where Nu_l is given by Eq. (6), Nu_t is given by Eq. (7), and the values of the constants a, b, and c for each inlet are as follows.

Reentrant:

$$a = 1766, \quad b = 276, \quad c = -0.955,$$

where

$$3 \le x/D \le 192, \quad 1700 \le \mathrm{Re} \le 9100, \quad 5 \le \mathrm{Pr} \le 51,$$
$$4000 \le \mathrm{Gr} \le 2.1 \times 10^5, \quad 1.2 \le \mu/\mu_w \le 2.2.$$

Square-edged:

$$a = 2617, \quad b = 207, \quad c = -0.950,$$

where

$$3 \le x/D \le 192, \quad 1600 \le \mathrm{Re} \le 10{,}700, \quad 5 \le \mathrm{Pr} \le 55,$$
$$4000 \le \mathrm{Gr} \le 2.5 \times 10^5, \quad 1.2 \le \mu/\mu_w \le 2.6.$$

Bell-mouth:

$$a = 6628, \quad b = 237, \quad c = -0.980,$$

where

$$3 \le x/D \le 192, \quad 3300 \le \mathrm{Re} \le 11{,}100, \quad 13 \le \mathrm{Pr} \le 77,$$
$$6000 \le \mathrm{Gr} \le 1.1 \times 10^5, \quad 1.2 \le \mu/\mu_w \le 3.1.$$

Equation (8) is applicable to transition forced and mixed convection in the entrance and fully developed regions and should be used with an appropriate set of constants for each inlet configuration. For the development of the transition region correlation for the reentrant inlet, 441 experimental data points were used. The correlation gave a representation of the experimental data to within +25.1% and −23% and had an absolute average deviation of 8%. Three percent of the data (13 data points) were predicted with more than ±20% deviation, 29% of the data (129 data points) with ±10–20% deviation, and 68% of the data (299 data points) with less than ±10% deviation. For the square-edged inlet, 416 experimental data points were used for the development of the correlation. The equation correlated the experimental data to within +24.3% and −23.9% and had an absolute average deviation of 7.2%. Three percent of the data (12 data points) were predicted with more than ±20% deviation, 26% of the data (106 data points) with ±10–20% deviation, and 72% of the data (298 data points) with less than ±10% deviation. The correlation for the bell-mouth inlet was based on 433 experimental data points. The correlation represented the experimental data to within +18.5% and −22% and had an absolute average deviation of 8.1%. Less than 1% of the data (four data points) were predicted with more than −20% deviation, 24% of the data (104 data points) with ±10–20% deviation, and 75% of the data (325 data points) with less than ±10% deviation.

PRACTICAL SIGNIFICANCE

Buoyancy influences forced convection heat transfer in horizontal pipes in ways that depend on the Reynolds, Prandtl, and Grashof numbers as well as on the type of pipe inlet configuration, wall boundary condition, and the length-to-diameter ratio of the pipe. The flow regime map provided in this study can be used to assist the heat exchanger designer in determining the influence of buoyancy in a horizontal circular tube with uniform wall heat flux for a specified inlet configuration in all flow regimes (laminar, transition, or turbulent). For the identified pure forced or mixed convection heat transfer regime, heat transfer calculations can be made based on the recommended correlations.

CONCLUSIONS

A new flow regime map for forced flow in a circular horizontal pipe with three different inlets under uniform wall heat flux is recommended. The flow regime map is unique in the sense that it is the first attempt at developing such a map for the case of a horizontal pipe with uniform wall heat flux. In the development of the flow regime map, particular attention was paid to the influence of inlet configuration on the start and end of the heat transfer transition region and the development of secondary flow along the pipe. Experimental data for three different inlet configurations (reentrant, square-edged, and bell-mouth) were used to verify the correctness of the map. The proposed map appears to be very general for the experimental data it was verified with and is applicable to both developing and fully developed flows. With a knowledge of Re and the parameter Gr Pr at a particular x/D location, the flow regime map can be used to identify the convection heat transfer flow regime (pure forced or mixed) for any of the three inlets. Once the convection heat transfer regime is established, correlations for calculation of heat transfer coefficient in the laminar, transition, and turbulent regimes are offered.

Support for this research was partially provided by the National Science Foundation under grant CBT-8813342.

NOMENCLATURE

- c_p specific heat of the test fluid evaluated at T_b, J/(kg K)
- D inside diameter of the test section (tube), m
- g acceleration of gravity, m/s^2
- h local average or fully developed peripheral heat transfer coefficient [$= \dot{q}_i''/(T_{wi} - T_b)$], W/(m^2 K)
- h_b local peripheral heat transfer coefficient at the bottom of the tube, W/(m^2 K)
- h_t local peripheral heat transfer coefficient at the top of the tube (180° from h_b), W/(m^2 K)
- h_x local peripheral heat transfer coefficient [$= \dot{q}_{ix}''/(T_{wix} - T_b)$], W/(m^2 K)
- Gr local bulk Grashof number [$= g\beta\rho^2 D^3(T_{wi} - T_b)/\mu^2$], dimensionless
- k thermal conductivity of the test fluid evaluated at T_b, W/(m K)
- L length of the test section (tube), m
- Nu local average or fully developed peripheral Nusselt number ($= hD/k$), dimensionless
- Nu_l local average or fully developed peripheral laminar Nusselt number, dimensionless

Nu_t local average or fully developed peripheral turbulent Nusselt number, dimensionless

Nu_{tr} local average or fully developed peripheral transitional Nusselt number, dimensionless

Nu_x local peripheral Nusselt number ($= h_x D/k$), dimensionless

Pr local bulk Prandtl number ($= \mu c_p/k$), dimensionless

$\dot{q}''_i$ local average peripheral inside wall heat flux, W/m^2

$\dot{q}''_{ix}$ local peripheral tube inside wall heat flux, W/m^2

Re local bulk Reynolds number ($= \rho VD/\mu$), dimensionless

St local average or fully developed peripheral Stanton number [$= Nu/(Pr\,Re)$], dimensionless

T_b local bulk temperature of the test fluid, °C

T_{wi} local average peripheral tube inside wall temperature, °C

T_{wix} local peripheral tube inside wall temperature, °C

V average velocity in the test section, m/s

x local distance along the test section from the inlet, m

Greek Symbols

β coefficient of thermal expansion of the test fluid evaluated at T_b, K^{-1}

μ absolute viscosity of the test fluid evaluated at T_b, Pa s

μ_w absolute viscosity of the test fluid evaluated at T_{wi}, Pa s

ρ density of the test fluid evaluated at T_b, kg/m^3

REFERENCES

1. Ghajar, A. J., and Tam, L. M., Heat Transfer Measurements and Correlations in the Transition Region for a Circular Tube with Three Different Inlet Configurations, *Exp. Thermal Fluid Sci.* **8**, 79–90, 1994.
2. Metais, B., and Eckert, E. R. G., Forced, Mixed and Free Convection Regimes, *Trans. ASME J. Heat Transfer* **10**, 295–296, 1964.
3. Kern, D. Q., and Othmer, D. F., Effect of Free Convection on Viscous Heat Transfer in Horizontal Tubes, *AIChE J.* **39**, 517–555, 1943.
4. Metais, B., Criteria for Mixed Convection, HTL Tech. Rep. No. 51, Heat Transfer Laboratory, Univ. Minnesota, Minneapolis, MN, 1963.
5. Ghajar, A. J., Strickland, D. T., and Kuppuraju, S., Forced and Mixed Convective Heat Transfer Measurements in a Circular Tube with Different Inlets, in *Mixed Convection*, R. L. Mahajan and R. D. Boyd, Eds., HTD-Vol. 152, pp. 37–45, ASME, New York, 1990.
6. Ghajar, A. J., and Zurigat, Y. H., Microcomputer-Assisted Heat Transfer Measurement/Analysis in a Circular Tube, *J. Appl. Eng. Educ.* 7(2), 125–134, 1991.
7. Sieder, E. N., and Tate, G. E., Heat Transfer and Pressure Drop in Liquids in Tubes, *Ind. Eng. Chem.* **28**, 1429–1435, 1936.
8. Eubank, O. C., and Proctor, S. M., Effect of Natural Convection on Heat Transfer with Laminar Flow, Thesis in Chemical Engineering, MIT, Cambridge, MA, 1951.
9. Chen, J., Heat Transfer in High Laminar, Transition and Lower Turbulent Flow Regimes for Square-Edged Contraction Entrance in a Circular Tube, Ph.D. Thesis, Oklahoma State Univ., Stillwater, OK, 1988.
10. Aung, W., Mixed Convection in Internal Flow, in *Handbook of Single-Phase Convective Heat Transfer*, S. Kakaç, R. K. Shah, and W. Aung, Eds., Chap. 15, p. 15-5, Wiley-Interscience, New York, 1987.

Received January 27, 1994; revised November 18, 1994